{DOTA-bis(amide)}lanthanide Complexes: NMR Evidence for Differences in Water-Molecule Exchange Rates for Coordination Isomers

Shanrong Zhang,[a] Zoltan Kovacs,[a] Shawn Burgess,[a] Silvio Aime,[c] Enzo Terreno,[c] and A. Dean Sherry*[a, b]

Abstract: Two derivatives of 1,4,7,10-tetraazacyclododecane with *trans*-acetate and *trans*-amide side-chain ligating groups have been prepared and their complexes with lanthanide cations examined by multinuclear NMR spectroscopy. These lanthanide complexes exist in aqueous solution as a mixture of slowly interconverting coordination isomers with ^{1}H chemical shifts similar to those reported previously for the major (**M**) and minor (**m**) forms of the tetraacetate ([Ln(dota)]$^-$) and tetraamide ([Ln(dtma)]$^{3+}$) complexes. As in the [Ln(dota)]$^-$ and [Ln(dtma)]$^{3+}$ complexes, the **m**/**M** ratio proved to be a sensitive function of lanthanide size and temperature. An analysis of ^{1}H hyperfine shifts in spectra of the Yb^{3+} complexes revealed significant differences between the axial (D_1) and non-axial (D_2) components of the magnetic susceptibility tensor anisotropy in the **m** and **M** coordination isomers and the energetics of ring inversion and **m** $\Leftrightarrow$ **M** isomerization as determined by two-dimensional exchange spectroscopy (EXSY). ^{17}O shift data for the Dy^{3+} complexes showed that both have one inner-sphere water molecule. A temperature-dependent ^{17}O NMR study of bulk water linewidths for solutions of the Gd^{3+} complexes provided direct evidence for differences in water exchange rates for the two coordination isomers. The bound-water lifetimes (τ_M^{298}) in the **M** and **m** isomers of the Gd^{3+} complexes ranged from 1.4 – 2.4 μs and 3 – 14 ns, respectively. This indicates that 1) the inner-sphere water lifetimes for the complexes with a single positive charge reported here are considerably shorter for both coordination isomers than the corresponding values for the [Gd(dtma)]$^{3+}$ complex with three positive charges, and 2) the difference in water lifetimes for **M** and **m** isomers in these two series is magnified in the [Gd{dota-bis(amide)}] complexes. This feature highlights the remarkable role of both charge and molecular geometry in determining the exchange rate of the coordinated water.

Keywords: lanthanides · macrocyclic ligands · NMR spectroscopy · water exchange

Introduction

The trivalent lanthanide ions (Ln^{3+}) provide a versatile series of spectroscopic probes for biological experiments, including applications as MRI contrast agents,[1, 2] NMR shift reagents,[3, 4] in vivo temperature reporters,[5–7] luminescent probes,[8, 9] and RNA cleavage catalysts.[10] There is considerable interest in using macrocyclic-based ligands (L) in these applications because of the high thermodynamic stability and kinetic inertness of the resulting [LnL] complexes. Two interesting physical features of many lanthanide complexes ([LnL]) derived from 1,4,7,10-tetraazacyclododecane (cyclen) are the presence of two stereochemical isomers (designated the major (**M**) and minor (**m**) isomers in studies of the [Ln(dota)]$^-$ complexes; DOTA = 1,4,7,10-tetraazacyclododecane-1,4,7,10-tetraacetic acid) and the differences in water exchange rates for cyclen derivatives with different coordinating side-arms. [Gd(dota)]$^-$, for example, has a single inner-sphere-bound water molecule that exchanges relatively rapidly with bulk water ($\tau_M^{298} = 244$ ns as measured by ^{17}O NMR).[11] This parameter is considered fundamental in optimizing the relaxivity of MRI contrast agents because transfer of proton relaxation between water bound at the paramagnetic center and bulk water should not be limited by exchange. Conversely, the water relaxivity of [Gd(dtma)]$^{3+}$ (in which DTMA is the **t**etra-substituted *N*-**m**ethyl **a**mide of DOTA) is limited by slow exchange of a single inner-sphere water molecule ($\tau_M^{298} = 19$ μs).[12] Water exchange in [Gd{dtpa-bis(methylamide)}] (DTPA = diethylenetriamine-*N*,*N*′,*N*″,*N*‴-pentaacetic acid) is also much slower[11] than in [Gd(dtpa)]$^{2-}$, so this appears to be a general feature of complexes that

[a] Prof. A. D. Sherry, S. Zhang, Z. Kovacs, S. Burgess
Department of Chemistry, University of Texas at Dallas
PO Box 830688, Richardson, TX 75083 (USA)
Fax: (+1) 972-883-2925
E-mail: sherry@utdallas.edu

[b] Prof. A. D. Sherry
Department of Radiology, Rogers Magnetic Resonance Center
5801 Forest Park Road, Dallas, TX 75235 (USA)

[c] Prof. S. Aime, E. Terreno
Dipartimento di Chimica IFM, Università di Torino
Via P. Giuria 7, 10125, Torino (Italy)

0947-6539/01/0701-0288 $ 17.50+.50/0

contain amide side-chain ligating groups. Since water exchange in these complexes occurs by a dissociative mechanism, the simplest explanation for these differences is that the water exchange rate decreases with the inverse of the overall complex charge, with positively charged systems like $[Gd(dtma)]^{3+}$ displaying much slower water exchange than negatively charged systems like $[Gd(dota)]^-$. However, more recently Aime et al.[13] reported that water exchange is about 50 times faster in the twisted, square antiprismatic isomer (**m**) than in the isomeric square antiprismatic (**M**) complex of identically charged lanthanide tetraamide complexes. This indicates that factors other than the charge of the complex play a role in determining the water exchange rate in lanthanide macrocyclic complexes. Separate ^{17}O resonances for bound water were also recently observed for $[Eu(dotam)]^{3+}$ (DOTAM is the simple **t**etra**am**ide of dota) and a reanalysis of water exchange in this system revealed that molecular exchange (as reported by ^{17}O NMR spectroscopy) and prototropic exchange (as reported by ^1H NMR spectroscopy) were equivalent for these complexes in acetonitrile.[14] Again, water exchange was found to be 40-fold faster in the **m** isomer compared with the **M** isomer ($\tau_M^{298} = 3$ μs vs 120 μs, respectively). More recently, Woods, et al.[15] studied a series of diastereomeric gadolinium complexes of the DOTA-tetra(carboxyethyl) derivative and found that the *R*,*R*,*R*,*R* complex stereoisomer existed predominately as the **m** isomer, whereas the *R*,*S*,*R*,*S* complex was largely the **M** isomer. Here, as with $[Gd(dota)]^-$, ^{17}O NMR linewidth data alone could not distinguish differences in water exchange rates for the two isomers, but empirical fit of the rates along with an independent measure of isomer populations led to the conclusion that the bound-water lifetime for the **m** isomer was constant ($\tau_m^{298} \approx 45$ ns) for a series of DOTA-type complexes.

In an effort to explore how complexes that contain ligands which differ only in the type of side-chain donor might alter water exchange and isomer populations, we synthesized two new cyclen-based macrocyclic derivatives containing two acetate- (like DOTA) and two amide-ligating (like DOTAM and DTMA) side chains. The synthetic route to such mixed side-chain systems has been reported previously.[16] Reported here are the results of multinuclear (^1H, ^{13}C, and ^{17}O) NMR studies of lanthanide complexes of the two bis-amide derivatives DOTA-2DMA and DOTA-2APA.

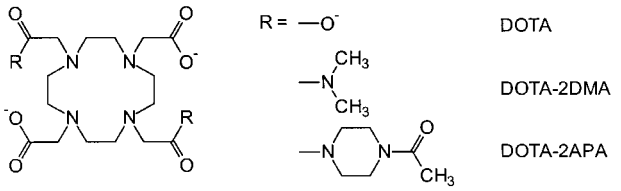

Results and Discussion

High-resolution NMR spectra of the $[Ln(dota\text{-}2dma)]^+$ complexes: The ^1H NMR spectrum of $[Ce(dota\text{-}2dma)]^+$ showed 14 well-resolved resonances (Figure 1), characteristic of a single complex with effective C_2 symmetry. The ^1H resonances in spectra of the Pr^{3+}, Nd^{3+}, and Sm^{3+} complexes were broad, while the spectrum of $[Eu(dota\text{-}2dma)]^+$ showed two sets of relatively sharp resonances, characteristic of two isomeric species in slow exchange. This last feature, also characteristic of the parent tetraacetate (DOTA)[15, 17–22] and tetraamide (DTMA) lanthanide complexes,[12, 13] was seen for all of the remaining heavier $[Ln(dota\text{-}2dma)]^+$ complexes (see for example the spectrum of $[Yb(dota\text{-}2dma)]^+$ in Figure 2). The ^1H resonances of $[Pr(dota\text{-}2dma)]^+$ and $[Nd(dota\text{-}2dma)]^+$ narrowed somewhat upon cooling to $-10\,^\circ C$ (data not shown), while ^1H spectrum of $[Sm(dota\text{-}2dma)]^+$ (with 6–7 broad peaks at 25 °C) collapsed into ~20 sharper peaks at $-10\,^\circ C$ (Figure 1). This indicates that a mixture of isomers is indeed present in all $[Ln(dota\text{-}2dma)]^+$ complexes (as observed directly for the heavier Ln complexes), but that chemical exchange among them appears to be a sensitive function of cation size, converging from rapid interconversion between isomers in $[La(dota\text{-}2dma)]^+$ to slow exchange in $[Eu(dota\text{-}2dma)]^+$.

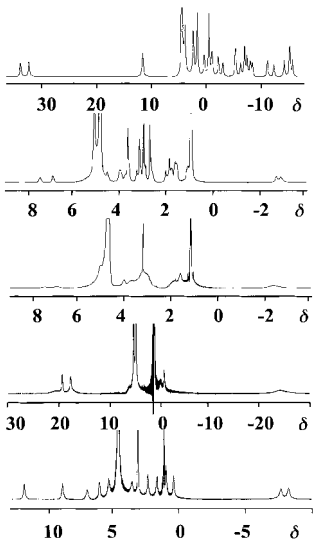

Figure 1. ^1H NMR spectra of $[Eu(dota\text{-}2dma)]^+$ (25 °C), $[Sm(dota\text{-}2dma)]^+$ ($-10\,^\circ C$), $[Sm(dota\text{-}2dma)]^+$ (25 °C), $[Pr(dota\text{-}2dma)]^+$ (25 °C), and $[Ce(dota\text{-}2dma)]^+$ (25 °C), top to bottom.

The high-frequency regions of the ^1H NMR spectra of the Eu^{3+} and Yb^{3+} complexes of DOTA-2APA, DOTA-2DMA, and DOTA are compared in Figure 2. The two hyperfine-shifted resonances shown in the spectra of $[Eu(dota)]^-$ and $[Yb(dota)]^-$ have been assigned to ethylene protons positioned near the fourfold symmetry axis[17] (previously designated as H4)[18] in two, slowly interconverting, coordination isomers. The H4 resonances of the major (**M**) and minor (**m**) isomers are labeled in the spectra. Hyperfine-shifted resonances were also observed in this same chemical shift region in the ^1H spectra of $[Eu(dota\text{-}2apa)]^+$, $[Eu(dota\text{-}2dma)]^+$, $[Yb(dota\text{-}2apa)]^+$, and $[Yb(dota\text{-}2dma)]^+$. The remaining resonances in these spectra displayed a chemical shift pattern similar to those in spectra of $[Eu(dota)]^-$ and $[Yb(dota)]^-$, complicated of course by the twofold symmetry of the bis-acetate/bis-amide substituents. Interestingly, two H4 resonances were resolved in the spectrum of the **M** isomer (as

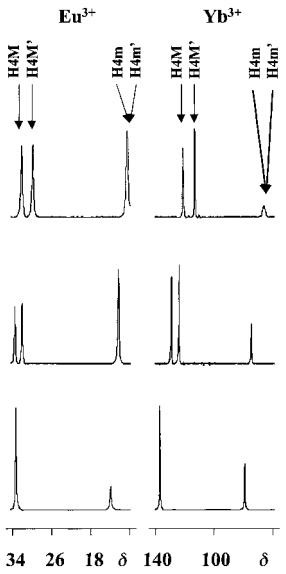

Figure 2. High-frequency regions of the ^{1}H NMR spectra of two [Ln(dota-2dma)]$^+$, [Ln(dota-2apa)]$^+$, and [Ln(dota)]$^-$ complexes (top-to-bottom) recorded at 25 °C. (Eu^{3+}, left; Yb^{3+}, right). The H_4 resonances of the **M** and **m** isomers are labeled (**M**, **M′** and **m, m′** identify degeneracies lifted by the twofold axis of symmetry in the bis-amide complexes).

expected for a complex with twofold symmetry), while the two H4 resonances of the **m** species are nearly coincident. This is especially evident in the spectrum of [Yb(dota-2apa)]$^+$ in which the H4 resonance of the **m** isomer is broader than the remaining resonances at 25 °C. The H4 resonances of the **m** species in all four samples could be resolved into two resonances upon cooling the samples to near 0 °C. The differences in magnetic degeneracy of the H4 resonances of the **M** and **m** species could have contributions from two sources. First, all protons experience smaller hyperfine shifts in the **m** isomer, so any magnetic difference between the two H4 protons is less evident than the H4 protons of the **M** isomer. Second, the coordinated acetate and amide oxygens in the **m** species are thought to have a smaller twist angle relative to the four nitrogens and thus the **m** isomer may more closely approximate axial symmetry (see hyperfine-shift section below).

The **m**/**M** species ratio in the spectrum of [Eu(dota)]$^-$ as measured by the H4 resonance areas (Figure 2) is 0.36, somewhat higher than the ratio reported elsewhere.[19–22] This ratio is known to be sensitive to ionic strength and can differ slightly from one sample preparation to another. Aime et al.[13] have recently shown that the **m**/**M** ratio increases in Eu^{3+} complexes of tetraamide derivatives of DOTA in proportion to the number of alkyl groups on the amide, increasing to **m**/**M** = 2 for the dimethylacetamide derivative. Their data show that as the steric bulk of the amide substituents increase, the twisted, square antiprismatic structure (**m**) becomes more favored. A similar trend is found here for the DOTA-bis(amide) systems. As shown in Figure 2 and reported in Table 1, the **m**/**M** ratio increases from 0.36 for [Eu(dota)]$^-$ to ~0.78 for the bis-amide complexes, [Eu(dota-2apa)]$^+$ and [Eu(dota-2dma)]$^+$. The observation that the **m**/**M** ratios for the two bis-amide ligand complexes are equal suggests that the steric demands of the dimethylamide (dma) and piperazineamide (apa) side chains are similar in these systems.

Table 1. Ratio of minor/major (**m**/**M**) isomers for two [Ln{dota-bis(amide)}]$^+$ complexes at 25 °C.

	Eu^{3+}		Yb^{3+}
	^{1}H NMR	^{13}C NMR	^{1}H NMR
DOTA-2DMA	0.77	0.64	0.25
DOTA-2APA	0.78	0.71	0.17
DOTA	0.36	0.30	0.54

The ^{13}C NMR spectra of these complexes (not shown) provide a second measure of the **m**/**M** isomer ratio. As expected, there are two carboxyl resonances in the spectrum of [Eu(dota)]$^-$ corresponding to the **m** ($\delta = 211$) and **M** ($\delta = 200$) isomers. In this case, the paramagnetic shift of the **m** species is larger than that of **M** species; this is likely due to a contact contribution at the ^{13}C nuclei that is less prominent at the ^{1}H nuclei. The ^{13}C spectra of [Eu(dota-2apa)]$^+$ and [Eu(dota-2dma)]$^+$ each show four carbonyl resonances in this region corresponding to the two carboxyl and amide groups in the major and minor isomers (the spectrum of [Eu(dota-2apa)]$^+$ has an additional carbonyl singlet from the uncoordinated acetyl groups). Again, the paramagnetic shifts (contact plus hyperfine) measured in the bis-amide complexes are somewhat smaller that those measured for [Eu(dota)]$^-$, and the δ chemical shift between the carboxyl and amide resonances in the **M** isomer is larger than in the **m** isomer. Integration of these peaks provided a second measure of **m**/**M** for the Eu^{3+} complexes (Table 1). A comparison of **m**/**M** ratios for each complex shows that the values determined by ^{1}H NMR spectra tend to be somewhat higher than the values determined by ^{13}C NMR spectra; this probably reflects nonuniform excitation of the most highly shifted resonances in the ^{1}H spectra. Nevertheless, it is quite clear from both sets of data that the **M** isomer dominates in [Eu(dota)]$^-$, while the **m** isomer is favored in both [Eu(dota-2apa)]$^+$ and [Eu(dota-2dma)]$^+$.

The most notable difference between the ^{1}H spectra of the Yb^{3+} and Eu^{3+} complexes is the **m**/**M** isomer ratio (see Figure 2). For the smaller Yb^{3+} ion, the **m** isomer is slightly more populated in [Yb(dota)]$^-$, but the **M** isomer predominates over the **m** isomer in both [Yb(dota-2apa)]$^+$ and [Yb(dota-2dma)]$^+$. In the mixed bis-amide systems, the **m**/**M** ratio averages 0.21 (Table 1). It has been suggested that the resonance corresponding to the **m** isomer of [Yb(dota)]$^-$ may actually be an eight coordinate species lacking a water molecule,[22] so it is possible that **m** species seen here in the ^{1}H spectra of [Yb(dota-2apa)]$^+$ and [Yb(dota-2dma)]$^+$ may also differ in structure from the **m** species detected in ^{1}H spectra of [Eu(dota-2apa)]$^+$ and [Eu(dota-2dma)]$^+$. The exact details of these structural elements must await crystallographic analysis of the species in question.

2D-EXSY NMR of [Eu(dota-2dma)]$^+$: 2D-EXSY spectra of [Eu(dota-2dma)]$^+$ proved useful in assigning the ^{1}H resonances and in measuring activation parameters for the intramolecular enantiomerizations. Similar techniques have been used to measure interchange between **m** ⇔ **M** isomers in ^{1}H

0947-6539/01/0701-0290 $ 17.50+.50/0 *Chem. Eur. J.* **2001**, *7*, No. 1

spectra of $[Yb(dota)]^-$.[20, 24] A 2D-EXSY spectrum of [Eu(dota-2dma)]$^+$ (0.2 M) collected at 20 °C and with a mixing time of 20 ms is shown in Figure 3. The spectrum shows many off-diagonal peaks, but the easiest to analyze for our purposes

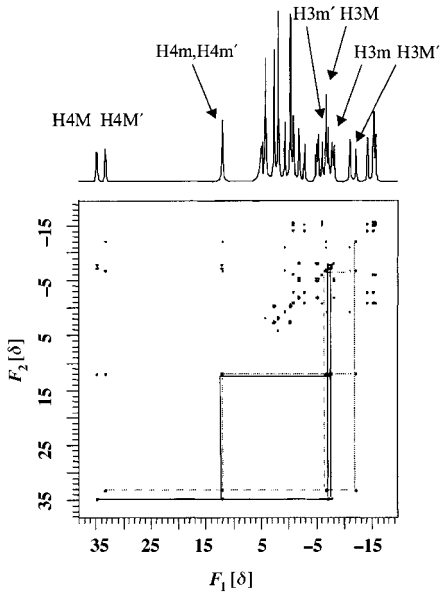

Figure 3. 2D-EXSY spectrum of [Eu(dota-2dma)]$^+$ at 500 MHz, 20 °C, ~0.2 M, and pH 7.2. $\tau_{mix} = 20$ ms, 32×256 scans, the data matrix was zero-filled to $1\,K \times 1\,K$. The corresponding cross peaks can be found for all exchange subgroups. For clarity, only {H4**M**, H4**m**, H3**M** and H3**m**} (solid line) and {H4**M′**, H4**m′**, H3**M′** and H3**m′**} (dotted line) were connected to guide the eye.

were those due to exchange between H4**M** ⇔ H4**m** (which reflects arm rotations of the acetate and amide groups) and H3**M** ⇔ H4**M** (which reflects enantiomerization due to ethylene ring inversions plus arm rotations). Of the less highly shifted ring proton resonances, the resonance assigned to H3 is well resolved from the others in this region. The cross-peak volumes of H4**M′** ⇔ H4**m′** and H4**M′** ⇔ H3**M′** are shown as a function of mixing time (20 °C) in Figure 4. As a first

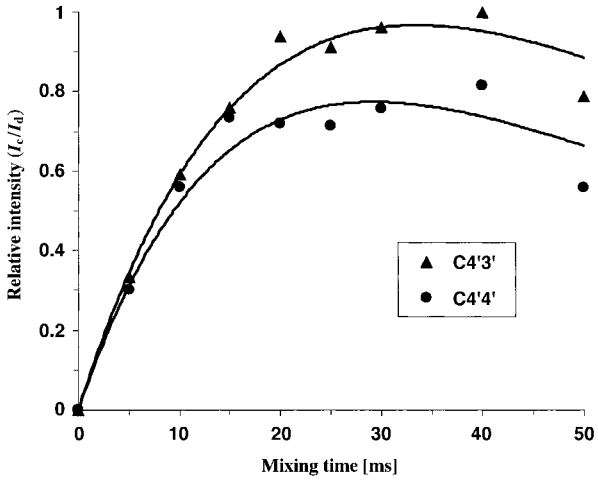

Figure 4. The curves of the relative intensities of I_c/I_d versus the mixing time at 20 °C for [Eu(dota-2dma)]$^+$, where C4′4′ and C4′3′ represent for the cross peaks of H4M′ ⇔ H4m′ and H4M′ ⇔ H3M′, respectively.

approximation, the cross (I_c) and diagonal (I_d) peak intensities are related to the mixing time (τ_{mix}), the relaxation time of exchanging nucleus (T_1), and the exchange rate (k_{ex}) by Equation (1).

$$\frac{I_c}{I_d} \propto [1 - \exp(-2 k_{ex} \tau_{mix})] \exp\left(-\frac{\tau_{mix}}{T_1}\right) \quad (1)$$

The kinetic parameters determined by fitting data such as those shown in Figure 4 are listed in Table 2. The free energy of activation for arm rotation and enantiomerization, $\Delta G^{\ddagger} = 66.0 \pm 2.5$ and 64.6 ± 3.4 kJ mol^{-1}, respectively, were found to

Table 2. Kinetic parameters (298 K) for [Eu(dota-2dma)]$^+$ derived from 2D-EXSY NMR spectra.

Process	ln*A* [kJ mol^{-1}]	E_a [kJ mol^{-1}]	$\Delta H^{\ddagger}$ [kJ mol^{-1}]	$\Delta S^{\ddagger}$ [J K^{-1} mol^{-1}]	$\Delta G^{\ddagger}$ [kJ mol^{-1}]
arm rotation	27.2	60.5	58.0	−26.7	66.0
enantiomerization	34.5	77.1	74.6	33.3	64.7

be nearly equal and similar to those reported previously for [La(dota)] (60.7 ± 1.2 kJ mol^{-1}, enantiomerization),[17] [Yb(dota)] (65.1 ± 0.8 kJ mol^{-1}, enantiomerization and 65.7 ± 1.3 kJ mol^{-1}, arm rotation),[24] and [La(dota-dea)]$^{3+}$ (58.5 kJ mol^{-1}, enantiomerization; DOTA-DEA is the tetrakis**die**thyl**a**mide of DOTA).[25] Interestingly, the activation energy for enantiomerization in [Eu(dota-2dma)]$^+$ is slightly lower than that for arm rotation, opposite that found[24] for $[Yb(dota)]^-$. The enantiomerization and arm rotation rates for [Eu(dota-2dma)]$^+$ were 29 and 17 s^{-1}, respectively, at 25 °C.

Analysis of the ^{1}H hyperfine shifts of [Yb(dota-2dma)]$^+$: The hyperfine ^{1}H NMR shifts observed for Yb^{3+} complexes are considered to be largely pseudocontact in origin,[26] so structural information can be derived by fitting the observed shifts to the dipolar Equation (2),

$$\Delta^i_{pc} = \frac{1}{2N}\left[(\chi_{zz} - 1/3\,Tr\chi)\left\langle\frac{3\cos^2\theta - 1}{r^3}\right\rangle + (\chi_{xx} - \chi_{yy})\left\langle\frac{\sin^2\theta\cos 2\varphi}{r^3}\right\rangle\right] + \frac{1}{N}\left[\chi_{zz}\left\langle\frac{\sin^2\theta\sin 2\varphi}{r^3}\right\rangle + \chi_{xz}\left\langle\frac{\sin^2\theta\cos\varphi}{r^3}\right\rangle + \chi_{xy}\left\langle\frac{\sin^2\theta\sin\varphi}{r^3}\right\rangle\right] \quad (2)$$

in which r, θ, and φ are the spherical coordinates of the ith nucleus in the molecular coordinate system with the Yb^{3+} ion located at the origin, χ is the magnetic susceptibility tensor, and $Tr\chi = \chi_{xx} + \chi_{yy} + \chi_{zz}$. For clarity, the molecular coordinate system was converted into the principal magnetic axis system by diagonalizing the χ susceptibility matrix into axial ($D_1 = \chi_{xx} - 1/3 Tr\chi$) and non-axial ($D_2 = \chi_{xx} - \chi_{yy}$) terms. The diamagnetic component of each shift was assumed to be constant (an average value of 3 ppm was used for all diamagnetic shifts upon complexation by La^{3+} or Lu^{3+}). Many resonances in the ^{1}H NMR spectrum of [Yb(dota-2dma)]$^+$ could be assigned by direct comparison with those of $[Yb(dota)]^-$ or with those of [Eu(dota-2dma)]$^+$ based upon the EXSY spectra discussed above, while others could not be assigned by simple inspection. A complete assignment was achieved by using the Shift Analysis technique described by Forsberg et al.[25] Molecular

mechanics calculations (MM+) were performed after fixing the Yb^{3+}–$O_{carboxyl}$ bond lengths to 2.279 Å as found experimentally[22] for [Lu(dota)]$^-$ and the Yb^{3+}–O_{amide} (2.355 Å), the Yb^{3+}–N (2.633 Å), and Yb^{3+}–O_{water} bond lengths (2.427 Å) to those reported[13] for [Dy(dtma)]$^{3+}$ (a tetraamide system). All remaining atomic bond lengths and angles in the molecule were allowed to vary during energy minimization, essentially following the procedure outlined in Forsberg, et al.[25] By using this procedure, two minimum energy structures were found, one corresponding to the square antiprism (**M**) structure and another to the twisted square antiprism (**m**). The coordinates of all protons in each structure were then entered into the Shift Analysis program and the resonance assignments were reshuffled to give the best agreement between calculated and observed hyperfine shifts.

We first tested the method by generating proton coordinates for the **m** and **M** structures of [Yb(dota)]$^-$. Comparisons were done by using [Yb(dota)]$^-$ hyperfine shifts from the literature (from ^{1}H spectra recorded at $-2\,^\circ$C)[17] and from our own data (from ^{1}H spectra recorded at 25 °C). An analysis of the hyperfine shifts recorded at $-2\,^\circ$C[17] gave D_1 values of 4022 and 2585 for the **M** and **m** isomers, respectively, and D_2 values near zero, as expected for complexes with axial symmetry. The hyperfine shift analysis performed by Brittain and Desreux[19] using earlier published crystal coordinates[27] of [Eu(dota)]$^-$ gave agreement factors ($R = [\Sigma(\Delta_{calcd} - \Delta_{obs})^2/\Sigma\Delta_{obs}^2]$) of 3.6% and 11% for the **M** and **m** isomers, respectively, while our analysis of their data gave much better agreement factors, R = 0.19% and 0.58% for **M** and **m**, respectively. This indicates that the crystal coordinates of [Eu(dota)]$^-$ do not serve as useful reference points for the structure of [Yb(dota)]$^-$ in solution and that the coordinates generated by MM+ minimization better describe the hyperfine shifts. A discrepancy between two different published crystal structures of [Eu(dota)]$^-$ has been recently noted.[28]

An assignment of all ^{1}H resonances of [Yb(dota-2dma)]$^+$, and a comparison of the measured versus calculated shifts by using the combined MM+ and Shift Analysis method is presented in Table 3. As found in the [Yb(dota)]$^-$ analysis, there was excellent agreement for both the **M** and **m** isomers of [Yb(dota-2dma)]$^+$ (R = 0.48% and 0.47%, respectively). Although the axial D_1 term dominates the hyperfine shift for most protons near the twofold symmetry axis of these complexes, the non-axial D_2 term is quite significant for others, especially the H5 and H6 protons. Interestingly, the D_2 term has opposite signs for the two isomers (D_2 is -1213 for the **M** isomer and $+926$ for the **m** isomer).

Table 3. Experimental and predicted ^{1}H chemical shifts for [Yb(dota-2dma)]$^+$.

	M isomer		**m** isomer	
	LIS[a] (exptl)	LIS[a] (calcd)	LIS[a] (exptl)	LIS[a] (calcd)
H1	−28.5	−24.1 ± 2.6	−19.0	−14.3 ± 1.7
H1′	−73.4	−64.5 ± 2.6	−46.5	−41.8 ± 1.6
H2	19.6	20.4 ± 1.6	12.2	15.3 ± 1.0
H2′	13.2	7.0 ± 1.9	0.8	2.3 ± 1.0
H3	24.7	25.4 ± 1.6	10.4	11.0 ± 1.0
H3′	16.6	13.8 ± 1.6	10.8	13.0 ± 1.0
H4	125.4	128.5 ± 2.9	72.4	71.8 ± 1.6
H4′	120.8	116.6 ± 2.8	72.4	73.4 ± 1.6
H5	−58.8	−63.7 ± 2.7	−52.3	−55.0 ± 1.9
H5′	−74.9	−81.1 ± 2.4	−49.0	−51.5 ± 1.9
H6	−40.0	−39.8 ± 1.7	−18.5	−16.3 ± 1.0
H6′	−33.3	−33.5 ± 1.8	−34.7	−31.5 ± 1.0
D_1	3807.1 ± 65.4		2409.9 ± 38.6	
D_2	−1212.7 ± 68.5		925.9 ± 42.5	
R	0.0048		0.0047	

[a] LIS = lanthanide-induced shift.

Water coordination number of [Dy(dota-2dma)]$^+$ and [Dy(dota-2apa)]$^+$: It has been shown[29] that the ^{17}O shift of bulk water in the presence of a Dy^{3+} complex, assuming rapid exchange, can provide a direct readout of the number of inner-sphere water molecules (q). Plots of ^{17}O shifts versus complex concentration were linear over the concentration range 5–50 mM (data not shown), and the slopes of such plots divided by the contribution of a single water molecule (40 ppm M^{-1})[29] indicated that $q = 1.3 \pm 0.1$ for both [Dy(dota-2dma)]$^+$ and [Dy(dota-2apa)]$^+$ at 25 °C. Titrations performed at higher temperatures (50 °C) gave identical values, thus proving that the value of q determined in this experiment was not limited by exchange at 25 °C. Furthermore, this result indicates that the **M** ⇔ **m** interconversion does not affect the q value suggesting that both isomers in the Dy^{3+} complexes have a single inner-sphere water molecule. A q value significantly greater than 1 was also been reported[29] for [Dy(dota)]$^-$ and attributed to a non-zero dipolar contribution to the measured ^{17}O contact shift.

^{17}O linewidth analysis of [Gd(dota-2dma)]$^+$ and [Gd(dota-2apa)]$^+$: The temperature dependence of the paramagnetic contribution to the ^{17}O water transverse relaxation rate (R_{2p}) of [Gd(dota-2dma)]$^+$ and [Gd(dota-2apa)]$^+$ are reported in Figure 5 (top). The shape shown by these profiles is very different from those reported previously[13–15, 30] for related Gd^{III} chelates, for which smooth curves are more typically seen. Given that high-resolution ^{1}H NMR spectra of the [Ln(dota-2dma)]$^+$ and [Ln(dota-2apa)]$^+$ complexes show that two isomers coexist in solution in similar amounts, is it easy to ascribe the shapes of the profiles shown in Figure 5 (top) to two isomeric species endowed with very different exchange lifetimes. Further support for this model was gained by measuring the proton relaxivity (r_1) of the two Gd^{3+} complexes as a function of the temperature (Figure 5, bottom). For both chelates the resulting profiles are far from the regular pseudoexponential decay expected for systems containing one coordinated water molecule in fast exchange with the bulk solvent. It is straightforward to suggest that the two species present in solution are the **m** and **M** isomers observed in the ^{1}H NMR spectra of the corresponding Eu and Yb analogues. Further support comes from recent observations made on the NMR spectra of [Eu^{III}(dota-tetrakis(amide)] derivatives in CD_3CN (for which it has been possible to observe the signals of the coordinated water molecules);[13, 14] these have shown that the twisted antiprismatic isomer (**m**) has a water exchange lifetime significantly shorter than that seen for the antiprismatic isomer (**M**).

Before carrying out a detailed analysis of the variable-temperature ^{17}O R_{2p} data on the basis of contributions from

0947-6539/01/0701-0292 $ 17.50+.50/0 *Chem. Eur. J.* **2001**, *7*, No. 1

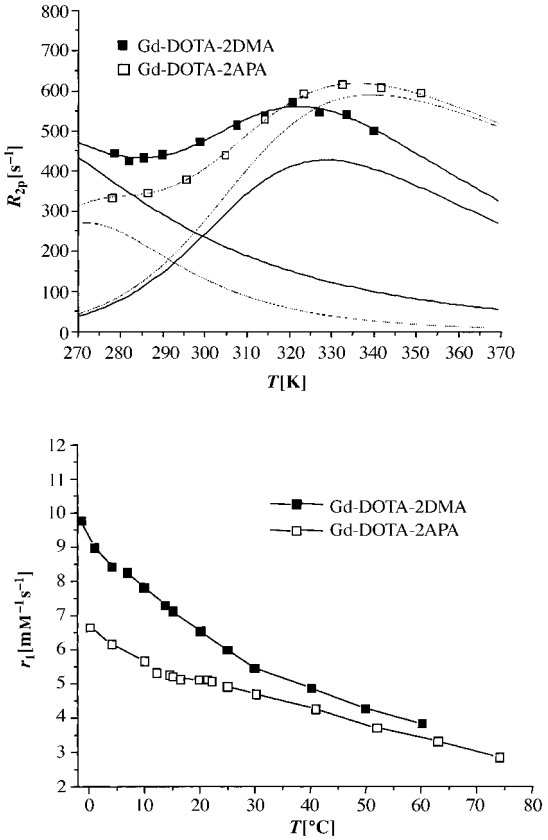

Figure 5. Temperature dependence of the ^{17}O water linewidth (top), R_{2P}, and the ^{1}H water relaxivity (bottom), r_1, of [Gd(dota-2dma)]$^+$ and [Gd(dota-2apa)]$^+$ at 2.1 T and 0.47 T, respectively.

the two isomers, it is necessary to include the temperature dependence of the **m**/**M** ratio. The **m**/**M** ratio (as measured by ^{1}H NMR) of each EuL complex ranged from $\sim$0.83 (5 °C) to$\approx$0.69 (60 °C). By using these data and Equation (3), ΔH^{o} was estimated at -2.56 kJ mol^{-1}.

$$K_T=\frac{[\mathbf{m}]}{[\mathbf{M}]}=K_{298}\exp\left[\frac{\Delta H^{o}}{R}\left(\frac{1}{298}-\frac{1}{T}\right)\right] \tag{3}$$

Then, the measured R^{o}_{2p} values ($R^{o}_{2p}=R^{o}_{2obs}-R^{o}_{2d}$) were treated as the sum of two contributions arising from the **m** and **M** isomers at the molar concentration given by Equation (4):

$$R^{2p}_{o}=\frac{q_1[\mathbf{M}]}{55.6}(\tau^{M\mathbf{M}}_{o})^{-1}\frac{R^{2M\mathbf{M}2}_{o}+\tau^{M\mathbf{M}}_{o})^{-1}R^{2M\mathbf{M}}_{o}+\Delta\omega^{M\mathbf{M}2}_{o}}{[R^{2M\mathbf{M}}_{o}+\tau^{M\mathbf{M}}_{o})^{-1}]+\Delta\omega^{M\mathbf{M}2}_{o}}$$
$$+\frac{q_1[\mathbf{m}]}{55.6}(\tau^{M\mathbf{m}}_{o})^{-1}\frac{R^{2M\mathbf{m}2}_{o}+\tau^{M\mathbf{m}}_{o})^{-1}R^{2M\mathbf{m}}_{o}+\Delta\omega^{M\mathbf{m}2}_{o}}{[R^{2M\mathbf{m}}_{o}+\tau^{M\mathbf{m}}_{o})^{-1}]+\Delta\omega^{M\mathbf{m}2}_{o}} \tag{4}$$

in which R^{2Mi}_{o} and $\Delta\omega^{2Mi}_{o}$ ($i=\mathbf{M}$ or $\mathbf{m}$) represent the transverse relaxation rate and the chemical shift difference (with respect the bulk water) of the metal-bound water molecule. The first term is dominated by the nucleus-electron scalar relaxation mechanism that may be evaluated through Equation (5):

$$R^{o}_{2Mi}=\frac{1}{3}\left(\frac{A}{\hbar}\right)^2 S(S+1)\left(\tau_{E1i}+\frac{\tau E2i}{1+\omega_s^2\tau^2_{E2i}}\right) \tag{5}$$

in which S is the electronic spin quantum number (7/2 for Gd^{III}), $A/\hbar$ is the Gd-^{17}O scalar coupling constant and τ_{Eji} ($j=1,2$) are the correlation times for the dynamic processes that modulate the scalar interaction. The scalar interaction can be described by the longitudinal and the transverse electronic relaxation times (T_{1Ei} and T_{2Ei}) modulated by the exchange lifetime of the metal bound water molecule [Eq. (6)].

$$\tau^{-1}_{Eji}=\tau^{o}_{Mi}{}^{-1}+T^{-1}_{jEi} \tag{6}$$

The scalar coupling constant is related to the electron unpaired spin density at the ^{17}O nucleus and mainly depends on the distance between the metal ion and the metal bound ^{17}O nucleus. Since this distance does not seem to vary significantly for polyaminocarboxylate Gd^{III} chelates with a single inner-sphere water molecule, we used the $A/\hbar$ value reported for [Gd(dota)]$^-$ (-3.8×10^6 rad s^{-1})[31] for both isomers (**m** and **M**).

For Gd^{III} complexes T_{jEi} is basically related to the modulation of the transient zero-field splitting (ZFS) of the electronic spin states arising from dynamic distortions of the ligand field caused by the solvent collisions. This can be described by Bloembergen-Morgan-Rubinstein theory as given in Equations (7) and (8).

$$T^{-1}_{1Ei}=\tfrac{1}{25}\Delta_i^2[4S(S+1)-3]\left[\frac{\tau_{vi}}{1+\omega_s^2\tau^2_{vi}}+\frac{4\tau_{vi}}{1+4\omega_s^2\tau^2_{vi}}\right] \tag{7}$$

$$T^{-1}_{2Ei}=\tfrac{1}{50}\Delta_i^2[4S(S+1)-3]\left[3\tau_{vi}+\frac{5\tau_{vi}}{1+\omega_s^2\tau^2_{vi}}+\frac{2\tau_{vi}}{1+4\omega_s^2\tau^2_{vi}}\right] \tag{8}$$

Here Δ_i^2 is related to the square of the mean transient ZFS energy, τ_{vi} is the correlation time for the collision-related modulation of the ZFS hamiltonian and ω_s is the electronic Larmor frequency.

The temperature dependence of R^{o}_{2Mi} is, therefore, expressed by the temperature effect on τ^{o}_{Mi}, τ_{vi} , and ω^{o}_{Mi} according to Equations (9) and (10).

$$\tau^{-1}_{ki}=\frac{(\tau_i^{-1})^{298.15}}{298.15}T\exp\left[\frac{\Delta H_{ki}}{R}\left(\frac{1}{298.15}-\frac{1}{T}\right)\right] \tag{9}$$

$$\Delta\omega^{o}_{Mi}=\frac{g_e\mu_B S(S+1)B}{3k_BT}\frac{A}{\hbar} \tag{10}$$

Here the subscripts k refer to the two dynamic processes ($k=M, v$), ΔH_{ki} is their activation enthalpy, B is the magnetic field strength, k_B is the Boltzmann constant, g_e is the free-electron Landè factor (2.0023), and μ_B is the Bohr magneton.

Given the large number of the parameters involved in the fitting of the ^{17}O R_{2p} data, we found it necessary to fix some of them. In particular, it was assumed that the two isomers have the same value of q (= 1), of ΔH_{vi} (10 kJ mol^{-1}), and of ΔH_{Mi} (50 kJ mol^{-1}). With these constraints, the result of the fitting procedure is quite satisfactory. As shown in Table 4, the most

Table 4. Relaxometric parameters for **M** and **m** isomers for the [Gd{dota-bis(amide)}]$^+$ complexes as determined from ^{17}O NMR line-shape analysis.

Parameter	[Gd(dota-2dma)]$^+$		[Gd(dota-2apa)]$^+$	
	M isomer	**m** isomer	**M** isomer	**m** isomer
τ^{298}_{M} [ns]	1350 ± 70	14.2 ± 1.0	2350 ± 120	3.0 ± 0.5
$\Delta^2\times10^{19}$ [s^{-2}]	1.1 ± 0.5	0.6 ± 0.1	0.8 ± 0.2	1.8 ± 0.7
τ_v [ps]	9.7 ± 1.0	2.0 ± 0.2	5.3 ± 0.2	3.6 ± 0.2
T_{1e} at 2.1 T [ns]	26.6	17.5	22.0	7.6

important result is the large difference (ca. two orders of magnitude) in the water exchange lifetime for the two isomers. Furthermore, it is interesting to point out that the **M** isomers of both [Gd{dota-bis(amide)}] complexes have longer T_{1E} values [calculated at 2.1 T through Eq. (8)] than the corresponding **m** isomers. It is likely that such an effect reflects the structural differences of the coordination cage of the two isomers, yielding a longer T_{1E} for the more compact **M** isomer.

This analysis leads to two main conclusions: i) as in the [Gd{dota-tetrakis(amide)}] systems,[13, 14] it is the **m** isomer which shows faster water exchange and ii) the ratio of water exchange rates for the two isomers in the [Gd{dota-tetrakis(amide)}] systems (~40-fold in CD_3CN[13, 14]) seems to be magnified in the [Gd{dota-bis(amide)}] complexes considered in this work (100- to 780-fold). Once again it is worth noting that this finding is highly relevant to the design of more powerful Gd^{III}-based contrast agents for MRI application whose proton relaxivity can be limited by a relatively long exchange lifetime of the coordinated water molecule.[31]

Finally, it may be of interest to evaluate the practical limitations in assessing different exchange lifetimes in the presence of an isomeric mixture. On the basis of a number of simulations (not shown), one can easily show that the ^{17}O R^{o}_{2p} measurements are sensitive to the presence of isomers with different water exchange lifetimes only if the isomeric ratio is higher than 0.3 (assuming water exchange in the dominant isomer is 100-fold faster). Conversely, if the **m**/**M** ratio ~1, then it is possible to discriminate water exchange lifetimes only if they differ by at least two orders of magnitude.

Conclusion

The $[Ln\{dota\text{-}bis(amide)\}]^{+}$ complexes, like the $[Ln(dota)]^{-}$ and $[Ln\{dota\text{-}tetrakis(amide)\}]^{3+}$ complexes, exist in solution as a mix of two structural coordination isomers, presumably the same square antiprism (**M**) and twisted square antiprism (**m**) structures as detected in solution and found in the solid state for $[Ln(dota)]^{-}$ complexes. As with the $[Ln(dota)]^{-}$ and $[Ln\{dota\text{-}tetrakis(amide)\}]^{3+}$ complexes, the **m**/**M** isomer ratio for these complexes is a sensitive function of Ln^{3+} cation size (the **m** isomer is favored with the larger Ln^{3+} cations, while the **M** isomer is favored for the smaller cations)[22] and steric bulk of the ligand side-chains (greater steric bulk favors the **m** isomer).[13] Previous ^{17}O NMR temperature-dependent linewidth measurements on Gd^{3+} complexes with tetraacetate DOTA-like ligands and tetrakisamide DOTAM-like ligands yielded smooth curves that did not directly reveal differences in water exchange rates for the **m** and **M** isomers. However, unusually slow water-exchange kinetics in some of the tetrakisamide complexes has permitted direct detection of bound water signals and this provided the first direct evidence for differences in water exchange rates for the two coordination isomers.[13, 14, 32] Since that remarkable observation, the temperature-dependent ^{17}O NMR linewidth data has been reevaluated in the context of two distinctly different exchange rates for water molecules. That reanalysis has revealed that the water exchange rates in the **m** and **M** species of $[Gd(dotam)]^{3+}$ differ by ~40 to 50-fold. In the mixed bis-acetate bis-amide complexes reported here, the ^{17}O NMR linewidth data provided direct evidence for two species in solution endowed with very different exchange lifetimes. A combined fitting of the ^{17}O and ^{1}H water linewidths revealed that the difference in bound water lifetimes in the **m** (3–14 ns) and **M** (1.4–2.4 μs) species is greatly magnified in $[Gd(dota\text{-}2dma)]^{+}$ and $[Gd(dota\text{-}2apa)]^{+}$. Interestingly, the water lifetime of the **M** species in these complexes is about the same as that estimated recently for the **M** species in several [Gd(dota)]-like complexes.[15] However, the water lifetimes estimated in that study[15] were based upon the assumption that the difference in lifetimes for the **m** and **M** species is identical for [Gd(dota)]-like complexes and the more slowly exchanging $[Gd\{dota\text{-}tetrakis(amide)\}]^{3+}$ systems. If this assumption is correct, then substitution of two amides for two acetates has little effect on water exchange in the square antiprism structure (**M**), but actually increases the water exchange rate in the twisted square antiprism (**m**) structure. This leads to the conclusion that water exchange in these complexes is influenced less by complex charge (the [Gd(dota)]-like complexes are all negatively charged, whereas $[Gd(dota\text{-}2dma)]^{+}$ and $[Gd(dota\text{-}2apa)]^{+}$ carry a single positive charge) and more by coordination geometry. These observations suggest that it may ultimately prove possible to fine-tune water exchange in lanthanide complexes from a few nanoseconds to perhaps as long as milliseconds by designing ligands with multiple side-chain pendant arms with different coordination and steric properties.

Experimental Section

NMR measurements and data processing: Variable-temperature, proton-solvent longitudinal relaxation times were measured at 20 MHz at Torino on a Spinmaster spectrometer (Stelar, Mede(PV), Italy) by means of the inversion-recovery technique (16 experiments, four scans). The reproducibility in T_1 measurements was within 1%. The temperature was controlled by a JEOL airflow heater equipped with a copper constantan thermocouple. The actual temperature in the probe head was measured with a Fluke 52k/j digital thermometer with an uncertainty of 0.5 K. Variable-temperature ^{17}O NMR measurements were performed on a JEOL EX-90 (2.1 T) spectrometer equipped with a 5 mm probe, by using a D_2O external lock. ^{1}H and ^{13}C NMR spectra were recorded on a Varian INOVA-500 spectrometer, with observing frequencies of 500 and 125.7 MHz, respectively. $^{1}H,^{1}H$ 2D-EXSY experiments were performed on the same spectrometer by using methods used previously.[19, 24] The mixing times (τ_{mix}) were varied from 0 to 100 ms by using 32 scans and 256 increments and the data were zero-filled to 1024×1024 for spectral processing. *tert*-Butyl alcohol (0.5% v/v) was used as internal reference for ^{1}H and ^{13}C spectra recorded in D_2O. Hyperfine paramagnetic shifts were analyzed using a program developed by Forsberg et al.[25] referred to in the text as Shift Analysis. Molecular mechanics minimizations (MMX) were performed by using the MM+ force field in HyperChem™ (release 5.01, Hypercube, Inc).

Complex preparation: Lanthanide complexes of DOTA-2DMA and DOTA-2APA were prepared by mixing a 1:1 molar ratio of $LnCl_3$ in water and the ligand in water followed by addition of NaOH to maintain pH between 7 and 8. The reaction mixtures were stirred at room temperature for a minimum of 24 hours until free Ln^{3+} ions could no longer be detected by using xylenol orange as indicator (in 0.2 M NaAc/HAc buffer solution at pH 5.2). The samples were then freeze dried to remove water and the resulting solid was redissolved in D_2O for NMR measurements.

0947-6539/01/0701-0294 $ 17.50+.50/0 *Chem. Eur. J.* **2001**, *7*, No. 1

Synthesis and characterization of ligands.

1-Acetyl-4-bromoacetyl piperazine: 1-Acetylpiperazine (1.0 g, 6.1 mmol) was dissolved in dichloromethane (100 mL). Diisopropylethylamine (1.1 g, 6.7 mmol, 10% excess) was added to the solution and the reaction vessel was cooled to −90 °C. Bromoacetylbromide (1.7 g, 5% excess) was dissolved in dichloromethane (10 mL) and added dropwise to the reaction vessel over 5 min. The reaction was allowed to warm to room temperature and then extracted with 10% HBr solution (3 × 10 mL). The dichloromethane phase was dried over sodium sulfate/potassium carbonate and decolorized with activated carbon. After filtering off the activated carbon, the solvent was removed under vacuum by rotary evaporation. The residue was washed with (3 × 20 mL) diethyl ether to yield a white powder (1.2 g, 79%). ^{1}H NMR ($CDCl_3$): $\delta = 3.90$ (br s, 2H; methylene protons), 3.65 (br m, 4H; $CH_3NCH_2CH_2N$), 3.54 (br m, 4H; $CONCH_2CH_2N$), 2.14 (s, 3H; methyl protons); ^{13}C NMR($CDCl_3$): $\delta = 169.18$ ($NCOCH_2Br$), 165.50 ($NCOCH_3$), 46.50, 46.23, 45.52, 45.74, 41.89, 41.72, 40.92, 40.70 (ring carbons), 25.38 ($NCOCH_2Br$), 21.14 ($NCOCH_3$); elemental analysis calcd (%) for $C_8H_{13}N_2BrO_2$: C 38.57, H 5.26, N 11.25; found: C 39.62, H 5.39, N 11.25.

4,10-Bis(1-acetyl-4-carbamoylmethylpiperazine)-1,7-bis(*tert*-butoxycarbonylmethyl)-1,4,7,10-tetraazacyclododecane: Di-*tert*-butyl 1,4,7,10-tetraazacyclododecane-1,7-diacetate (1.2 g, 3.0 mmol) was dissolved in anhydrous acetonitrile (20 mL). Potassium carbonate (3 g, 18 mmol, 350% excess) was suspended in the reaction solution. 1-Acetyl-4-bromoacetyl piperazine (1.52 g, 6.1 mmol, 2% excess) in acetonitrile (10 mL) was then added to the reaction vessel. The reaction was stirred at 40 °C for 24 h and 60 °C for 8 h. The potassium carbonate was filtered off and the solvent was removed by rotary evaporation. The residue was dissolved in dichloromethane (25 mL) and the solution was extracted with water (3 × 25 mL). The organic phase was dried over sodium sulfate for 24 h. The solvent was removed under vacuum to give 2.0 g of yellow solid. This crude product was loaded onto a neutral alumina column (200 g) and eluted with 2% methanol 98% acetonitrile. The fractions containing the pure product were combined, and the solvent removed to give colorless solid (1.8 g, 67%). ^{1}H NMR ($CDCl_3$): $\delta = 3.61$ (s, 2H; NCH_2CON), 3.43 (s, 2H; $CH_2COOtBu$), 3.52 (br, 16H; $CONCH_2CH_2NCO$), 2.82 (br, 16H; NCH_2CH_2N), 2.15 (s, 6H; CH_3), 1.46 (s, 18H; $C(CH_3)_3$); ^{13}C NMR($CDCl_3$): $\delta = 172.50$ (NCH_2COO-*tert*-butyl), 171.50, 169.31 ($NCOCH_3$), 52.51, 48.53 (macrocyclic ring carbons) 46.50, 46.23, 45.52, 45.74, 41.89, 41.72, 40.92, 40.70 (piperazine carbons), 25.38 ($C(CH_3)_3$), 21.14 ($NCOCH_3$); HRFAB: *m*/*z*: 759.4739 $[M+Na]^+$ (deviation = −0.8); elemental analysis calcd (%) for $C_{36}H_{64}N_8O_8 \cdot 2HBr$: C 48.11, H 7.40, N 12.47; found C 48.24, H 7.44, N 12.53.

4,10-Bis(1-acetyl-4-carbamoylmethyl-piperazine)-1,4,7,10-tetraazacyclododecane-1,7-diacetic acid (DOTA-2APA): 4,10-Bis(1-acetyl-4-carbamoylmethylpiperazine)-1,7-bis(*tert*-butoxycarbonylmethyl)-1,4,7,10-tetraazacyclododecane (1.0 g, 1.1 mmol) was placed into a 250 mL round-bottom flask and dissolved in HCl (6 M, 50 mL). This solution is stirred at room temperature for 0.5 h. The solvent was removed by rotary evaporation at 5 mbar, and the residue was placed under high vacuum to remove the excess HCl. The residue was partially dissolved in water (0.5 mL) and then completely dissolved by adding absolute ethanol (4 mL). Diethyl ether (200 mL) was added dropwise to this stirred solution to precipitate the product. The product was filtered under a nitrogen atmosphere to yield a white hygroscopic powder (0.9 g, 94%). ^{1}H NMR (D_2O): $\delta = 3.67$ (br, 8H; $COCH_2NCH_2CH_2NCH_2CON$), 3.65 (br, 4H; NCH_2COO), 3.63 (br, 4H; NCH_2CON), 3.55 (br, 8H; $COCH_2NCH_2CH_2NCH_2CON$), 3.49 (br, 2H; $CONCH_2CH_2NCO$), 3.37 (br, 2H; $CONCH_2CH_2NCO$), 3.15 (br, 2H; $CONCH_2CH_2NCO$), 3.07 (br, 2H; $CONCH_2CH_2NCO$), 2.15 (s, 3H; $NCOCH_3$); ^{13}C NMR (D_2O): $\delta = 175.33$ (NCH_2CON), 173.58 (NCH_2COO), 164.57 (br, $NCOCH_3$), 55.88 (br, NCH_2CON), 53.84 (NCH_2COO), 52.62, 48.65 (br, macrocyclic carbons), 46.21, 46.14, 44.76, 44.50, 42.65, 42.30, 41.88, 41.76 (piperazine carbons), 21.16 ($NCOCH_3$); HRFAB: *m*/*z*: 625.3672 $[M+H]^+$ (deviation = −0.2); elemental analysis calcd (%) for $C_{28}H_{48}N_8O_8 \cdot 2HBr \cdot 2HCl$: C 36.44, H 6.44, N 12.14, (Cl+Br) 25.00; found: C 36.53, H 6.26, N 12.11, (Cl+Br) 25.44.

1,7-Bis(*tert*-butoxycarbonylmethyl)-4,10-bis(dimethylcarbamoylmethyl)-1,4,7,10-tetraazacyclododecane: Di-*tert*-butyl 1,4,7,10-tetraazacyclododecane-1,7-diacetate (1.00 g, 2.5 mmol) was dissolved in anhydrous acetonitrile (10 mL) and potassium carbonate (1.5 g) was added. Bromoacetic acid dimethylamide was dissolved in acetonitrile (5 mL), and the solution was added to the reaction mixture in small portions. The mixture was stirred at 50 °C for two days. Acetonitrile was removed by rotary evaporation, and the residue was taken up in dichloromethane (20 mL). Potassium carbonate/potassium bromide was filtered off, and the solvent was removed by rotary evaporation. The yellow amorphous solid (1.70 g) crystallized upon treatment with diethyl ether (20 mL). The product was filtered on a Schlenk filter, washed with diethyl ether (3 × 10 mL) and dried in nitrogen stream to give a white powder (1.56 g, 90.7%). ^{1}H NMR ($CDCl_3$, 500 MHz): $\delta = 1.47$ (s, 18H; *t*Bu), 2.15 (br; NH^+), 2.93 (s, 6H; NCH_3), 2.99 (s, 6H; NCH_3), 2.6–3.6 (br, 16H; NCH_2); ^{13}C NMR ($CDCl_3$, 125 MHz): $\delta = 27.78$ (CCH_3), 35.19 (NCH_3), 36.24 (NCH_3), 49.10 (br, NCH_2), 52.12 (br, NCH_2), 55.29 (NCH_2CO), 56.78 (NCH_2CO), 81.37 ($OCCH_3$), 169.95 (CO), 171.82 (CO); elemental analysis calcd (%) for $C_{28}H_{54}N_6O_6 \cdot 1.47\ HBr$: C 48.76, H 8.11, N 12.19; found: C 48.79, H 8.04, N 12.12.

4,10-Bis(dimethylcarbamoylmethyl)-1,4,7,10-tetraazacyclododecane-1,7-diacetic acid (DOTA-2DMA): 1,7-bis(*tert*-butoxycarbonylmethyl)-4,10-bis(dimethylcarbamoylmethyl)-1,4,7,10-tetraazacyclododecane (1.00 g, 1.4 mmol) was dissolved in a small amount of water (2–3 mL) and 20% hydrochloric acid (10 mL) was added. After the mixture was stirred at room temperature for 1 h, the water/hydrochloric acid was removed by rotary evaporation at 5 mbar. The residue was taken up with diethyl ether (10 mL), filtered on a Schlenk filter, and dried in a stream of nitrogen to give a white solid (0.98 g, 99%). ^{1}H NMR (D_2O, 500 MHz): $\delta = 2.97$ (s, 6H; NCH_3), 2.99 (s, 6H; NCH_3), 3.11 (non-first-order multiplet, 8H; NCH_2), 3.52 (br s, 8H; NCH_2), 3.58 (br s, 4H; NCH_2CO), 4.38 (br s, 4H; NCH_2CO); ^{13}C NMR (D_2O, 125 MHz): $\delta = 37.06$ (NCH_3), 37.5 (NCH_3), 49.34 (NCH_2), 53.44 (NCH_2), 54.39 (NCH_2CO), 56.88 (NCH_2CO), 166.41 (CO), 175.21 (CO); elemental analysis calcd (%) for $C_{20}H_{38}N_6O_6 \cdot 1.47\ HBr \cdot 1.66\ HCl \cdot 2.43\ H_2O$: C 35.21, H 6.80, N 12.32; found: C 35.21, H 6.80, N 12.33.

Acknowledgements

This work was supported in part by grants to A.D.S. from the Robert A. Welch Foundation (AT-584), the National Institutes of Health (CA-84697), and the Division of Research Resources, National Institutes of Health (RR-02584).

[1] J. C. Bousquet, S. Saini, D. D. Stark, P. F. Hahn, M. Nigam, J. Wittenberg, J. T. Ferrucci, Jr., *Radiology* **1988**, *166*, 693–698.
[2] R. B. Lauffer, *Chem. Rev.* **1987**, *87*, 901–927.
[3] D. C. Buster, M. M. C. A. Castro, C. F. G. C. Geraldes, C. R. Malloy, A. D. Sherry, T. C. Siemers, *Magn. Reson. Med.* **1990**, *15*, 25–32.
[4] N. Bansal, M. Germann, V. Seshan, G. T. Shires III, C. R. Malloy, A. D. Sherry, *Biochemistry* **1993**, *32*, 5638–5643.
[5] S. Aime, M. Botta, M. Fasano, E. Terreno, P. Kinchesh, L. Calabi, L. Paleari, *Magn. Reson. Med.* **1996**, *35*, 648–651.
[6] K. Roth, G. Bartholomae, H. Bauer, T. Frenzel, S. Kossler, J. Platzek, B. Baduechel, H.-J. Weinmann, *Angew. Chem.* **1996**, *108*, 691–693; *Angew. Chem. Int. Ed. Engl.* **1996**, *35*, 655–657.
[7] C. S. Zou, J. L. Bowers, K. R. Metz, T. Nosaka, A. D. Sherry, M. E. Clouse, *Magn. Reson. Med.* **1996**, *36*, 955–959.
[8] D. Parker, K. Senanayake, J. A. G. Williams, *Chem. Commun.* **1997**, 1777–1778; D. Parker, K. Senanayake, J. A. G. Williams, *J. Chem. Soc. Perkin Trans. 2* **1998**, 2129–2139.
[9] D. Parker, J. A. G. Williams, *Chem. Commun.* **1998**, 245–246.
[10] S. Amin, J. R. Morrow, C. H. Lake, M. R. Churchill, *Angew. Chem.* **1994**, *106*, 824–826; *Angew. Chem. Int. Ed. Engl.* **1994**, *33*, 773–775.
[11] K. Micskei, L. Helm, E. Brucher, A. E. Merbach, *Inorg. Chem.* **1993**, *32*, 3844–3850.
[12] S. Aime, A. Barge, M. Botta, D. Parker, A. S. De Sousa, *J. Am. Chem. Soc.* **1997**, *119*, 4767–4768.
[13] A. Aime, A. Barge, J. I. Bruce, M. Botta, J. A. K. Howard, J. M. Moloney, D. Parker, A. S. De Sousa, M. Woods, *J. Am. Chem. Soc.* **1999**, *121*, 5762–5771.
[14] F. A. Dunand, S. Aime, A. E. Merbach, *J. Am. Chem. Soc.* **2000**, *122*, 1506–1512.
[15] M. Woods, S. Aime, M. Botta, J. A. K. Howard, J. A. Moloney, M. Navet, D. Parker, M. Port, O. Rousseaux, *J. Am. Chem. Soc.* **2000**, *122*, 9781–9792.

[16] Z. Kovacs, A. D. Sherry, *Synthesis* **1997**, 759 – 763.
[17] J. F. Desreux, *Inorg. Chem*. **1980**, *19*, 1319 – 1324.
[18] C. F. G. C. Geraldes, A. D. Sherry, G. E. Kiefer, *J. Magn. Reson*. **1992**, *97*, 290 – 304.
[19] H. G. Brittain, J. F. Desreux, *Inorg. Chem*. **1984**, *23*, 4459 – 4466.
[20] S. Aime, M. Botta, G. Ermondi, *Inorg. Chem*. **1992**, *31*, 4291 – 4299.
[21] M. P. M. Marques, C. F. G. C. Geraldes,A. D. Sherry, A. E. Merbach, H. Powell, D. Pubanz, S. Aime, M. Botta, *J. Alloys Compd.* **1995**, *225*, 303 – 307.
[22] S. Aime, M. Botta, M. Fasano, M. P. M. Marques, C. F. G. C. Geraldes, D. Pubanz, A. E. Merbach, *Inorg. Chem*. **1997**, *36*, 2059 – 2068.
[23] S. Aime, A. Barge, M. Botta, M. Fasano, J. D. Ayala, G. Bombieri, *Inorg. Chim. Acta* **1996**, *246*, 423 – 429.
[24] V. Jacques, J. F. Desreux, *Inorg. Chem*. **1994**, *33*, 4048 – 4053.
[25] J. H. Forsberg, R. M. Delaney, Q. Zhao, G. Harakas, R. Chandran, *Inorg. Chem*. **1995**, *34*, 3705 – 3715.
[26] A. D. Sherry, C. F. G. C. Geraldes in *Lanthanide Probes in Life, Chemical and Earth Sciences: Theory and Practice* (Eds.: J. -C. G. Bünzli, G. R. Choppin), Elsevier, Amsterdam, **1989**.
[27] M. R. Spirlet, J. Rebizant, J. F. Desreux, M. F. Loncin, *Inorg. Chem*. **1984**, *23*, 359 – 363.
[28] F. Benetollo, G. Bombieri, S. Aime, M. Botta. *Acta Crystallogr. Sect. C* **1999**, *55*, 353 – 356.
[29] M. C. Alpoim, A. M. Urbano, C. F. G. C. Geraldes, J. A. Peters, *J. Chem. Soc. Dalton Trans.* **1992**, 463 – 467.
[30] D. H. Powell, O. M. Ni Dhubhghaill, D. Pubanz, L. Helm, Y. S. Lebedev, W. Schlaepfer, A. E. Merbach, *J. Am. Chem. Soc*. **1996**, *118*, 9333 – 9346.
[31] S. Aime, M. Botta, M. Fasano, E. Terreno, *Chem. Soc. Rev*. **1998**, *27*, 19 – 29.
[32] S. Aime, A. Barge, M. Botta, A. S. De Sousa, D. Parker, *Angew. Chem.* **1998**, *110*, 2819 – 2820; *Angew. Chem. Int. Ed.* **1998**, *37*, 2673 – 2675.

Received: April 20, 2000 [F2437]

0947-6539/01/0701-0296 $ 17.50+.50/0